Estimating Soil Erosion Risk in District Diamer, Pakistan Using RUSLE Model: A Spatial Analysis Approach

Maria Anum[1], Arshad Ashraf[2], Kalim-Ullah[1], Durr-e-Adan[1], Muhammad Awais[3]
[1]Department of Meteorology, Comsats University Islamabad
[2]Principal Scientific Officer, National Agriculture Research Centre, NARC Park Road, Islamabad
[3]GIS Analyst, DHA Gujranwala, Gujranwala
*Correspondence: Marianjc7@gmail.com

Citation | Anum. M, Ashraf. A, Ullah. K, Adan. D. E, Awais. M, "Estimating Soil Erosion Risk in District Diamer, Pakistan Using RUSLE Model: A Spatial Analysis Approach", IJIST, Vol. 07 Special Issue. pp 218-236, August 2025
Received| July 25, 2025 **Revised|** August 12, 2025 **Accepted|** August 13, 2025 **Published|** August 14, 2025.

Soil erosion is a critical issue in the hilly regions of Diamer, Pakistan, due to the region's varying topography and significant precipitation patterns. This study uses an effective combination of Geographic Information System (GIS) technologies and the Revised Universal Soil Loss Equation (RUSLE) model to calculate soil erosion rates within the region's complex topography. Different GIS layers, such as rainfall erosivity (R), slope length and steepness (LS) factor, soil erodibility (K), conservation practices (P), and cover management factor (C), were merged by utilizing satellite data and the Normalized Difference Vegetation Index (NDVI). The resulting map showed a maximum soil loss of 2279.3 t/ha/year over the region. Notably, the greatest soil loss was observed in the western regions of Diamer, where rainfall and rainfall erosivity are also recorded as high in these areas. Five separate categories of soil erosion were identified, with a mean soil loss rate of 27 t/ha/year. According to the GIS analysis, 95% of the overall area experienced less severe erosion than the severe erosion classes, accounting for 5%. Additionally, the study included the computation of composite NDVI estimates for 2023 using Google Earth Engine (GEE). This method improved both the scalability and usability of the study by enabling effective processing and storage of data in the cloud. GEE enables the computation of NDVI quickly and precisely. This pioneering study is an important step toward understanding and resolving soil erosion issues in Diamer, Pakistan. The study offers valuable insights for decision-making and management planning initiatives by utilizing cutting-edge GIS tools and RUSLE modeling.

Keywords: Remote sensing, GIS, Soil Erosion, Revised Universal Soil Loss Equation, Land-use & Land-cover.

Introduction:

The natural geological process of soil erosion involves the removal and transportation of soil by wind, water, or gravity. The loss of topsoil due to erosion can have serious repercussions, such as reduced soil fertility, decreased crop yields, and increased water pollution, even though human activities like deforestation, crop cultivation, construction, and mining have significantly accelerated soil erosion rates [1]. Because soil erosion causes nutrients to detach from the topsoil, it negatively affects agricultural productivity. This effect increases the amount of silt that enters reservoirs, which reduces their active storage capacity. To mitigate the impacts of erosion-induced soil loss, an estimated 45% of India's Western Ghats and Himalayan areas require strategic planning and interventions for soil conservation [2]. Due to the high slopes and shifting farming practices in the northeastern Himalayas, it is estimated that more than 3 million hectares per year of agricultural soil are eroded each year [3]. Due to an acceleration of land degradation rates, climate change is impacting the soil and agricultural yields of semi-arid and desert agroecology [4].

The entire Himalayan region's soil erosion is influenced by the geology, climate, and land-use patterns of the basin, but human activity also has a significant impact [5]. The region has been affected by factors that increase soil erosion and silt concentration in the upper and lower Himalayan rivers, including deforestation, large-scale road construction, mining, and cultivation on steep slopes. These factors also increase the likelihood of larger floods, which carry extremely large sediment loads [6]. Soil erosion predictions and quantifications are limited in Pakistan at the national level due to several factors, such as topographical roughness, remoteness, and diversity, as well as a lack of data accessibility and processing capability. The annual amount of soil erosion varies from less than one to more than twenty tons per hectare. The yearly mean of soil erosion in the rugged highlands of the Gilgit region was high, 5–20 tons/ha/year, and very high, exceeding 20 tons/ha/year [7]. Ninety percent of the land of Gilgit Baltistan's topography consists of mountains, which are prone to landslides and the formation of lakes. The region is topographically rugged [8].

In Diamer District, the soil quality has been impacted by several human activities, such as deforestation, the transformation of pasturelands into agricultural land, and intensive farming methods. It was noted that the percentage of moisture and organic carbon in the agricultural soils was significantly reduced. As more areas are converted to agriculture, soil erodibility and degradation have increased. It was found that the agricultural soils had much lower percentages of moisture and organic carbon. As more land is converted to agriculture, there may be a corresponding increase in soil erodibility and degradation [9]. In the lower hundreds of kilometers of the upper Indus River valleys, downcutting, trenching, and aggradation epicycles have dominated deposition and erosion [10]. Due to its rugged topography, frequent seismic activity, and monsoon rains, northern Pakistan is home to a wide range of geo-hazards. Asia experiences the greatest losses in food production due to erosion and disturbance of the local forest-dependent communities [11].

There are multiple models available for predicting soil erosion based on empirical data (USLE/RUSLE), and their data inputs differ significantly. They project the impacts of raindrops on topography, climate, soil, and land use that affect soil erosion. This model is frequently used to calculate the risk and loss from soil erosion. It offers guidance for creating conservation strategies and managing erosion in various land cover types, including croplands, pastures, and degraded forest areas. To estimate soil erosion and determine its spatial distribution across larger areas, remote sensing and GIS approaches are practical. It is possible to quantify soil degradation at a cell-by-cell level by integrating remote sensing and GIS with the Universal Soil Loss Equation model [12].

Research Objective:

The main objectives of the present study are as follows:

To calculate the C-Factor based on NDVI.
To identify and assess areas prone to soil erosion.
To provide spatial and thematic maps of erosion-prone areas.
To develop strategies for long-term protection against future soil erosion.

Materials and Methods:

Study Area:

This study focused on the Diamer District in the Pakistani region of Gilgit Baltistan (Figure 1). Geographically, it is located at latitudes 35° 2' and 35° 50' North and longitudes 73° 6' and 74° 44' East. The region's elevation ranges from 2438.4 to 35,000 meters. On mild to moderate slopes, the soil is formed through rock dissolution and is loamy and fairly deep. The region experiences no more than 250 mm of precipitation annually due to its generally dry climate and arid environment. Most precipitation is received from December to May [13].

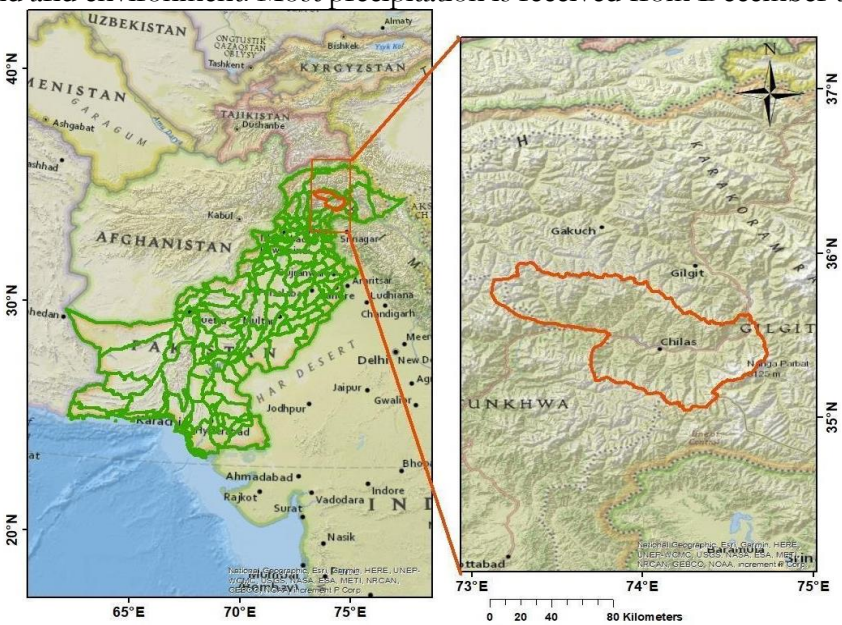

Figure 1. Study Area

Dataset:

The following datasets (Table 1) were utilized for the analysis from the mentioned sources: Rainfall data was collected from the Pakistan Meteorological Department (PMD). An interpolation method, namely Inverse Distance Weighted (IDW), was used to create a rainfall map for the study area based on the monthly average rainfall estimated from the data. The soil data was obtained from the Soil Survey of Pakistan, which includes 30 ground points, and the K factor has been calculated. The NASA SRTM Digital Elevation Model (DEM) at 30 m resolution was used for computing the LS factor. The Landsat 9 OLI dataset collection of the least cloudy images was filtered to produce the median composite for 2023. The product used is from the Level 1 collection, which means that image processing (geometric and radiometric corrections) has already been done on the data. Then, the NDVI index was computed to derive the C factor. The amount of time needed to retrieve, download, and prepare imagery is greatly reduced by using the GEE platform.

Table 1. Description of data

No	Data type	Source	Description
1	DEM	NASA / USGS / JPL-Caltech	NASA SRTM Digital Elevation 30m
2	Satellite	USGS/Google	USGS Landsat 9 imagery Collection 2 Tier 1 TOA Reflectance
3	Soil data	Soil survey of Pakistan	Includes 30 ground points

4	Rainfall data	Meteorological Department of Pakistan	Rain data for the period of 20 years (2000-2019)

Methodology:

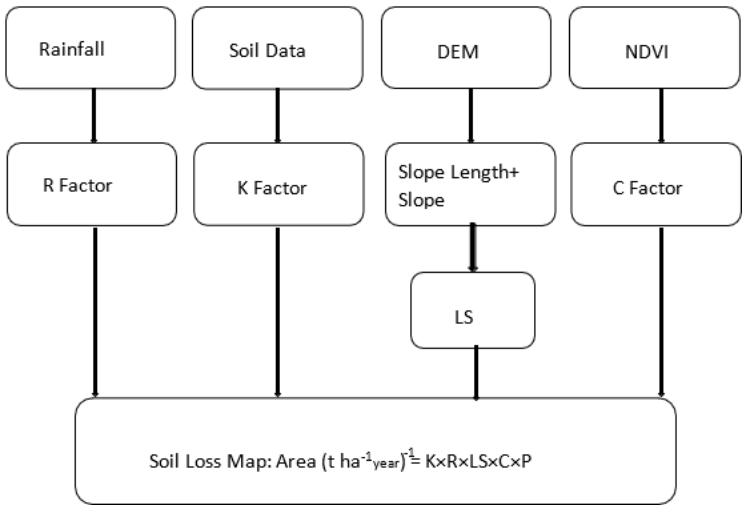

Figure 2. Methodology Chart

Universal Soil Loss Equation:

In this study, soil types, agricultural practices, and a land cover map were produced using remotely sensed satellite imagery to apply the RUSLE model. The model's primary feature, which makes it a suitable choice for this study, is its ease of incorporation into GIS for enhanced analysis. The methodology used for this study is shown in Figure 2. Five interconnected and time- and space-varying input factors were combined to create the Universal Soil Loss Equation. Each factor's input data is interdependent and subject to change across time and space, which results in the computation of erosion at the pixel level.

$$A = R \times K \times LS \times C \times P \quad (1)$$

Where A is the mean annual soil loss expressed in tons per hectare, and R is the rainfall and runoff factor expressed in megajoules per hectare per hour annually, are two of the factors included in the equation. K is the soil erodibility factor in tons per hectare per megajoule per mm; P is the conservation practice factor; C is the cover management factor; and LS is a dimensionless combination of slope length and steepness.

The impact of rainfall intensity on soil erosion is reflected in the erosivity of the rainfall factor (R), which expresses the erosivity of rainfall over a specific location based on the quantity and intensity of rainfall. The RUSLE's rainfall erosivity must describe the rate and quantity of runoff associated with rainfall and measure the impact of raindrops [14]. As the month-to-month data on precipitation are the most available**, the following formula is suitable** to calculate rainfall erosivity and erodibility as described by [15];

Where Pi is the monthly rainfall and P is the annual rainfall

The rate of soil erosion is represented by the soil erodibility factor. The permeability of the soil, its organic matter content, its texture, structure, and many other factors all affect the K factor. It is a measurement of the overall impact of a specific combination of soil properties. The following equation was applied [16].

$$Log\ R = 1.93 log \sum pi^2/p - 1.5 \quad (2)$$

$$KUSLE = fcsand \times fcl - si \times forgc \times fhisand \quad (3)$$

$$fcsand = \left\{0.2 + 0.3exp[-0.256ms]\left(1 - \frac{msilt}{100}\right)\right\} \quad (4)$$

$$fcl - si = \left(\frac{msilt}{mc+msilt}\right)^{0.3} \quad (5)$$

$$fcsand = 1 - \left\{\frac{0.0256\ orgC}{orgC + \exp[3.72 - 2.95 \cdot orgC)]}\right\} \quad (6)$$

$$fhisand = 1 - \left[\frac{0.7\left(1 - \frac{ms}{100}\right)}{\left(1 - \frac{ms}{100}\right) + exp\left[-5.51 + 22.9\left(1 - \frac{ms}{100}\right)\right]}\right] \quad (7)$$

The L and S parameters in the USLE show how topography affects the erosion rate. Greater flow over land and soil erosion are indicated by longer slopes and steeper slopes. Furthermore, compared to differences in slope length, slope variations produce a much greater effect on gross soil loss [17]. Topography plays a significant role, especially when the ground slope exceeds the critical angle. The DEM was used to obtain the LS factor. This is because the terrain's slope length and slope steepness, which are required inputs for computing the LS factor, are provided by the DEM. Variables like flow accumulation and slope steepness must be taken into consideration. The LS factor was calculated using the equation below as recommended by [18].

$$LS = Pow\ (([\text{Flow accumulation}] * \text{CellSize})/22.1,0.4)) * Pow(([sinSlope] * 0.01745)/0.09,1.4) * 1.4 \quad (3)$$

Where the slope degree is indicated by "sinSlope," whose value is in sine; flow accumulation indicates the amount of cumulative upslope contributing area for a cell; the LS factor provides the factor of the length of the slope along with slope steepness; and cell size shows the size of a grid cell.

The type and amount of vegetation cover have a significant impact on soil loss. In simple terms, vegetation cover absorbs the kinetic energy of raindrops before they reach the soil's surface, preventing raindrops from impacting the soil. According to [19], the type of vegetation, stage of growth, and percentage of vegetation cover all have a direct impact on the cover management factor (C), which indicates that the C factor can also be calculated by the NDVI used to quantify vegetation cover indicators. The range of the C-factor is 0 to 1 as suggested by [20], and it describes the amount of vegetation cover and the impact of crops on soil erosion. Vegetation coverage is thought to be essential for reducing water erosion. The relationship between soil erosion under specific vegetation and soil erosion on bare land is established by the NDVI. It also emphasizes how cover density and type affect soil preservation. The following equation was used to create a C-factor map as described by [21]. The estimation of the C factor from NDVI is a unique approach [22].

There are different formulas for calculating the C factor via NDVI; the following is the most suitable [23]. Using the JavaScript programming language in GEE, the Landsat 9 dataset collection of the least cloudy images was filtered to produce the median composite for 2023. Then, the NDVI index was computed to derive the C factor. The amount of time needed to retrieve, download, and prepare imagery is greatly reduced by using the GEE platform [24]

$$C = (-NDVI + 1)/2 \quad (3.10)$$

Where the curve shape for the NDVI and C factor is denoted by the unitless parameters α and β (α = 2 and β = 1) [25].

$$NDVI = \frac{NIR - Red}{NIR + Red} \quad (8)$$

Another name for the conservation practice factor (P) is the support practice factor. According to the Association of Agricultural Land, the support practice factor has a mathematical value between 0 and 1. It shows an optimal P factor when it is near zero, and an improper P factor when it is near one [1]. P-factor measurements for slope according to agricultural practices are provided by [26].

Results and Discussions:

To determine the erosion rate in the study area, the various components of the RUSLE

model were estimated. The annual rate of erosion was determined in tons per hectare per year using the RUSLE equation. The Raster Calculator, a tool in ArcGIS, was used to calculate and multiply the R, K, LS, and C factors to predict the rate of soil loss in the study region. More precise techniques for estimating soil erodibility (K), rainfall erosivity (R), cover management (C), and slope length and steepness (LS) are supported by the RUSLE model. Data collected on the various variables used to compute soil erosion will serve as a guide for developing suitable plans for land management and soil conservation. The study area's total amount of soil erosion loss, the severity of soil erosion's spatial distribution, and the locations of vulnerable sites are all estimated using RUSLE.

Rainfall Erosivity Factor:

The distribution pattern of annual rainfall is displayed in Figure 3. The values of annual rainfall were found to be 168 and 154, respectively. Diamer's yearly mean annual rainfall was 319. The distribution pattern of the annual R factor is displayed in Figure 4. The values of R were found to be a minimum of 23 and a maximum of 184, respectively. Diamer's yearly mean R was 53, with a standard deviation of 33. The district's western region has the highest values of rainfall and experiences high erosivity. The acceptance and accuracy of the IDW method for interpolation in producing annual rainfall spatial data led to its use.

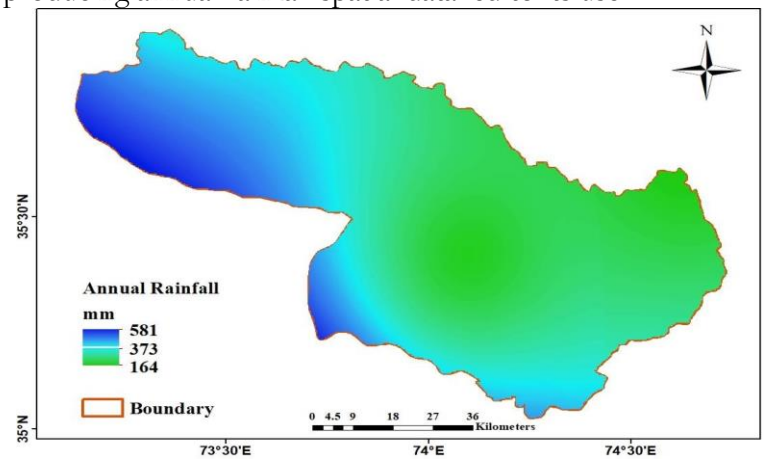

Figure 3. Annual Rainfall

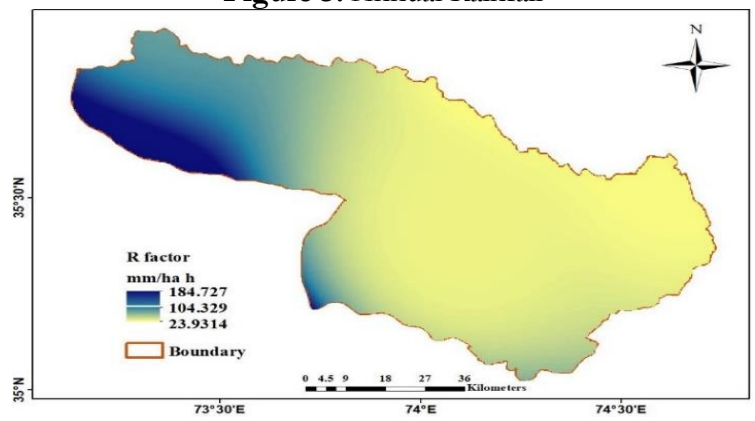

Figure 4. Rainfall erosivity

Soil Erodibility Factor:

Different soil types (Table 2) are more or less susceptible to erosion. The K factor, also known as soil erodibility, refers to the soil's inherent susceptibility to runoff and rainfall-induced soil erosion. Soil erodibility can be determined by a variety of physical and chemical properties. The main factors that influence the size of particles, soil composition, organic matter, and soil permeability are the physical characteristics of soil that the RUSLE model considers most important in determining soil erodibility. The K factor for the study was created using the soil

map (shown in Figure 5) that was obtained from the Soil Survey of Pakistan. The calculated K factor values demonstrated that, with an average of 0.159 tons ha h ha^{-1} MJ^{-1} mm^{-1}, K values range from 0.15 to 0.18 tons ha h ha^{-1} MJ^{-1} mm^{-1} (Figure 6).

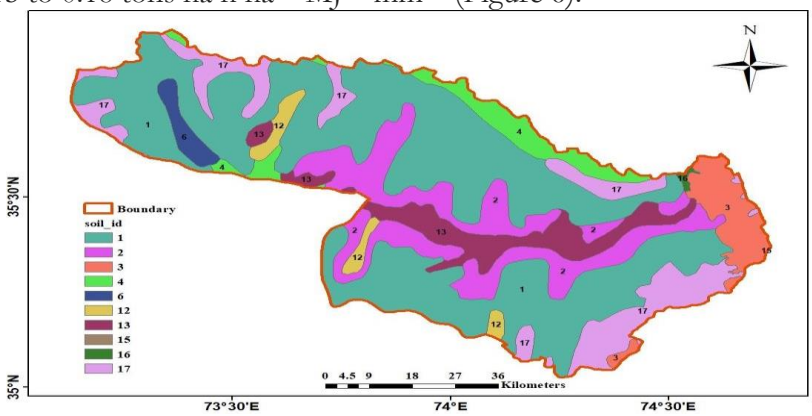

Figure 5. Soil Map

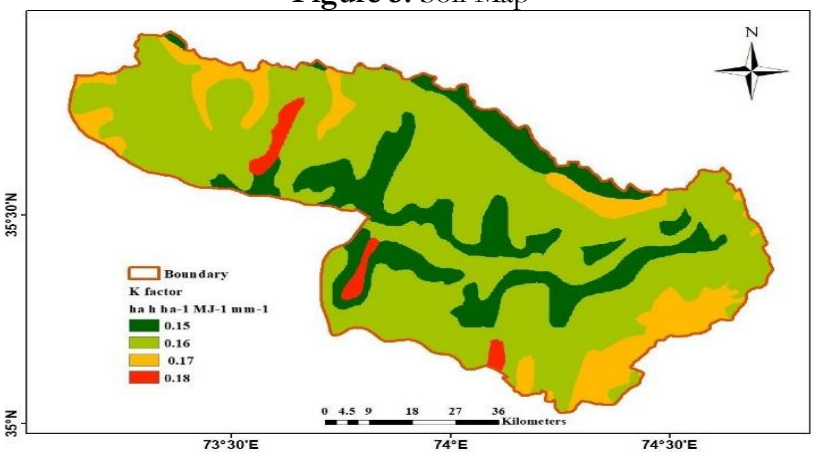

Figure 6. Soil erodibility map

Table 2. Major land types and soil mapping units recognized in the study area [27]

Soil ID	Land types/ Geomorphology	Soil characteristics
1	Mountain-Valley Systems	Shallow/moderately deep, non-calcareous, acid to slightly alkaline soils in the mountains and deep, non-calcareous, acid/ neutral, medium textured soils in the valleys
2	(Fair to good soil cover on mountain slopes)	Shallow/moderately deep, calcareous, slightly/moderately alkaline soils in the mountains and deep, mainly non-calcareous, slightly/moderately alkaline, medium textured soils in the valleys
3	(Patchy soil cover on mountain slopes)	Shallow/moderately deep, mostly non-calcareous, neutral/slightly alkaline soils in the mountains and deep, non-calcareous, neutral/ slightly alkaline, medium textured overlaying gravel/ stone bed in the valleys
4		Scattered, shallow/ very shallow, calcareous, moderately alkaline soils in the mountains and moderately deep, calcareous, moderately alkaline, medium textured soils in the valleys

5	Gravelly Fans	Gently sloping, shallow to moderately deep, non-calcareous, neutral/slightly alkaline, medium-textured soils overlying a gravel/stone bed.
6		Nearly level to gently sloping, shallow/moderately deep, calcareous, slightly/moderately alkaline, medium to coarse textured soils overlying a gravel/stone bed
7	Weathered Bedrock	Gently sloping, moderately deep/deep, non-calcareous, slightly alkaline, medium-textured soils
8	Loess deposits	Gently sloping, moderately deep, non-calcareous, neutral/slightly alkaline, mainly fine to moderately fine textured soils
9		Level to gently sloping, deep, calcareous, moderately alkaline, mainly medium, some moderately fine-textured soils.
10	Alluvial Basins/Valleys (Level/Nearly Level – Flat)	Deep, non-calcareous, slightly alkaline, mainly medium-textured, some coarse-textured soils
11		Deep, non-calcareous, slightly alkaline, mainly medium, some moderately fine-textured soils
12	(Nearly level/Gently sloping, locally dissected)	Deep, non-calcareous, acid/slightly alkaline, medium, partly coarse-textured soils
13		Deep, calcareous, moderately/slightly alkaline, medium to coarse textured soils
14		Moderately deep, calcareous, moderately alkaline, gravelly, coarse to medium textured soils
15	(Gently sloping, locally dissected)	Shallow/moderately deep, non-calcareous, acid/slightly alkaline, mainly medium-textured soils
16		Shallow/moderately deep, calcareous, moderately alkaline, mainly medium, some coarse-textured soils
17	Miscellaneous areas (Permanent snow/Glaciers)	The area comprising perennial snow or a large mass of ice mixed with earthy materials.
18	(Water body/ River course)	Lakes, reservoirs, wetlands, and river courses comprising an area subject to frequent reworking by a major river

Slope Length and Steepness Factor:

Topography affects soil erosion in a range that is determined by the USLE's LS factor, which describes the effects of the slope steepness factor S and length factor L. In general, when the length of the slope (L) increases, soil erosion increases, and the soil erosion area grows as a result of the dynamic accumulation of excess flow in the downslope path. In the event that the slope's steepness increases, both runoff and velocity increase. The slope (Figure 7) is measured in degrees and divided into four categories. The LS factor in this study is generated from the SRTM DEM, and its values range between 0 and 523 (Figure 8).

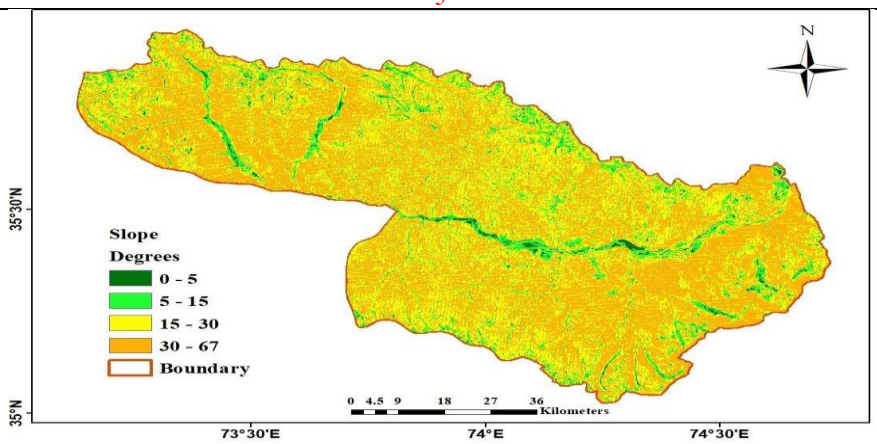

Figure 7. Slope map

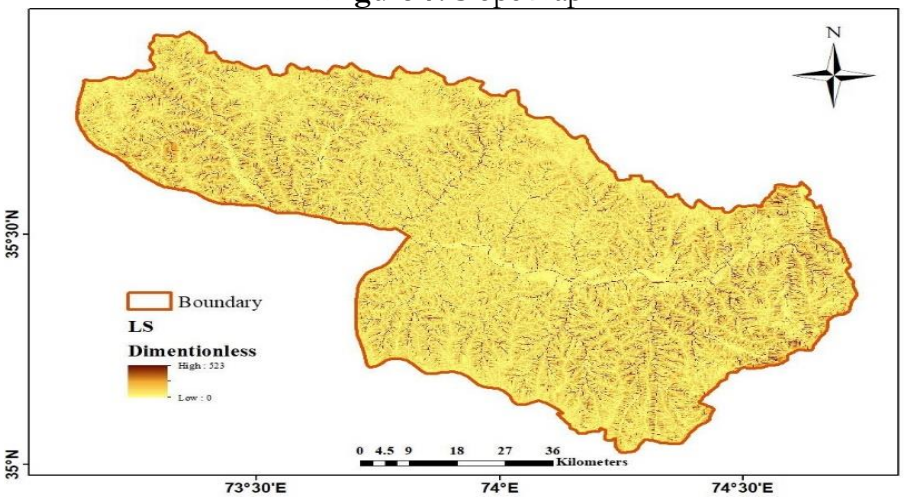

Figure 8. Slope length and slope steepness factor

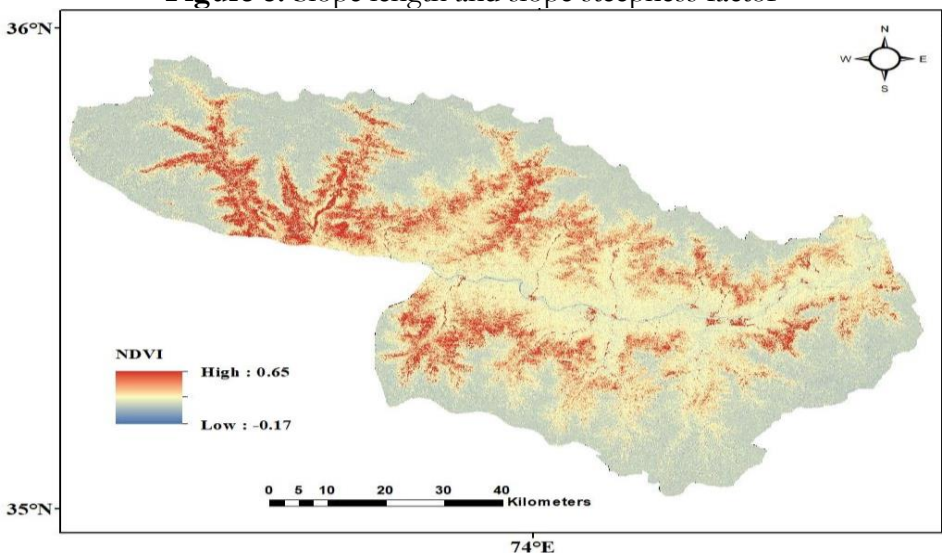

Figure 9. NDVI calculated from Sentinel-2

Cover Management Factor (C):

The calculated NDVI using Sentinel-2 imagery ranged between -0.17 and 0.65 (Figure 9). A higher value for the C factor indicates a water body or barren land, whereas a lower value indicates an area with high vegetation cover. The cover management factor is also calculated from LULC (Figure 10) and its values ranged from 0.001 to 0.2, while the C factor calculated from Sentinel-2 (Figure 11) ranged between 0.17 and 0.58. The mapping and computation of

the C factor were done using the yearly composite of the NDVI in 2023. The study area's NDVI values range from -0.35 to 0.6 (Figure 12). Using GEE, the C factor mapping and NDVI of the region were created. It was discovered that the C factor value ranges from 0.15 to 0.67 (Figure 13).

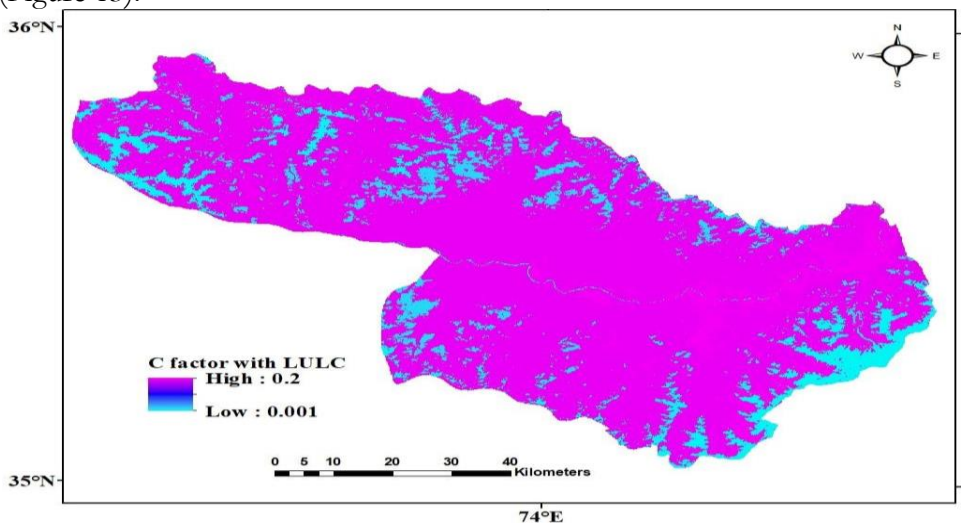

Figure 10. C factor calculated from LULC

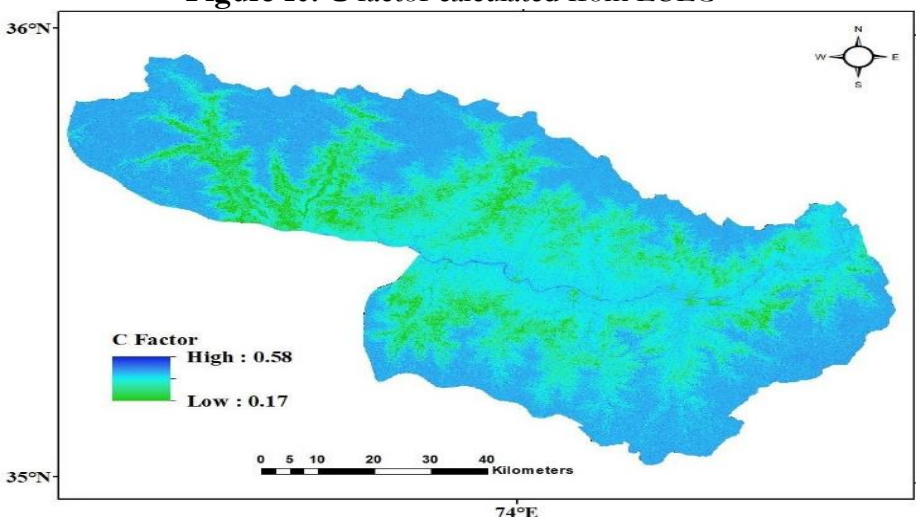

Figure 11. C factor from Sentinel-2 imagery

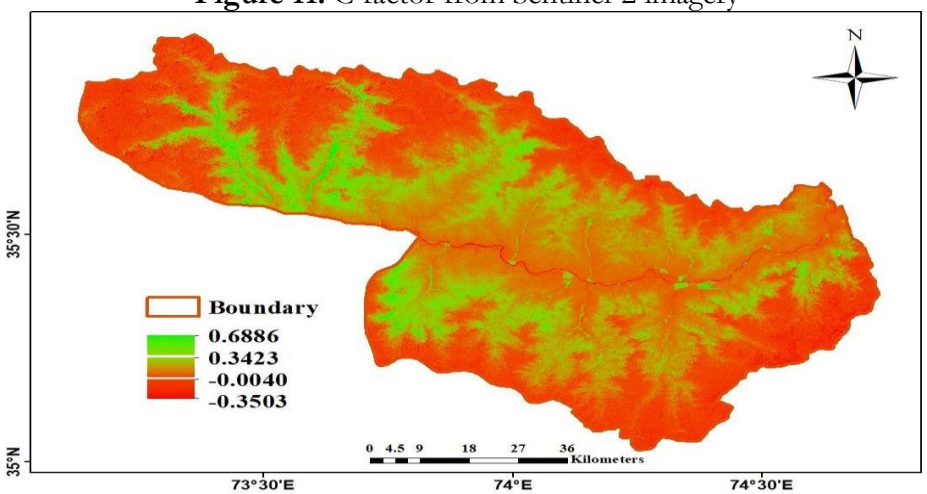

Figure 12. NDVI median composite of 2023

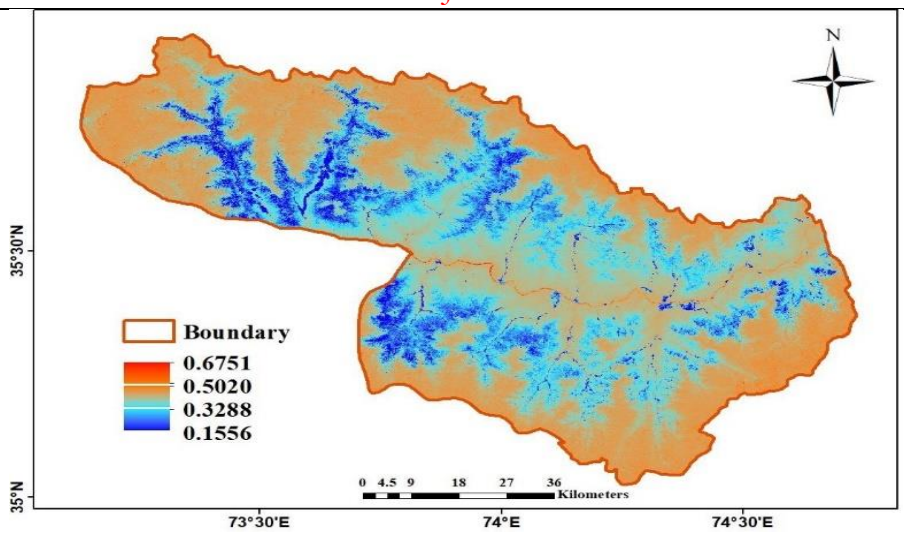

Figure 13. C factor calculated from Landsat imagery

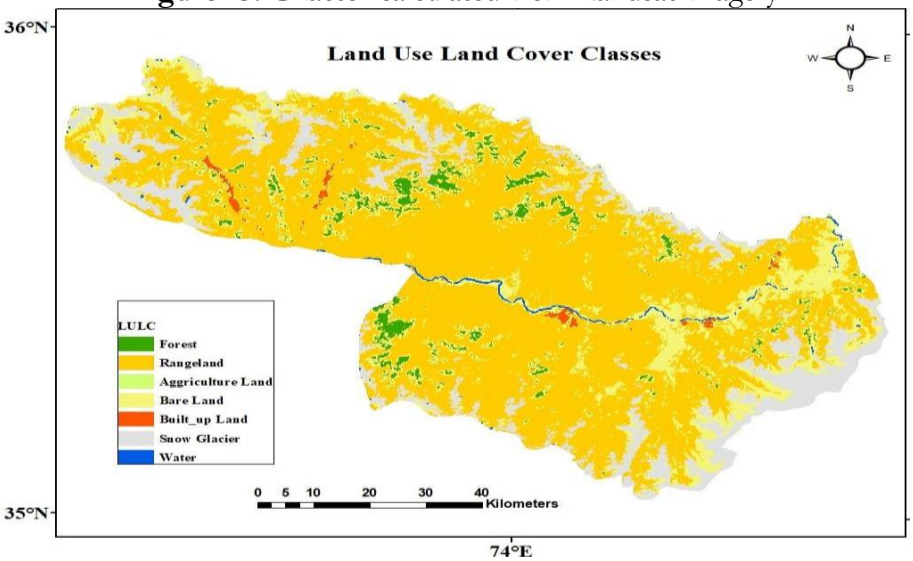

Figure 14. Land Use Land Cover

Using Sentinel-2 images from the European Space Agency (ESA) between 2017 and 2022, ESRI created a global LULC map. To analyze the distribution of land cover and vegetation in the area, the ESRI website (https://livingatlas.arcgis.com) provided the spatial data of land use/land cover (LULC) as shown in Figure 14. The impact of land use change on soil erosion and its interaction with climate change is well-established. However, because there are so many factors (such as socioeconomic, cultural, environmental, and political factors) that affect land use at all scales from local to global, predicting how land use will change in response to future climate conditions is not an easy task. Due to these complications, it is not surprising that the effect of climate change on soil loss is rarely examined in conjunction with changes in land use and vegetation development.

Estimation of Potential Erosion:

Increased soil erosion is predicted to result from climate change in many parts of the world, which will affect ecological services and human welfare. There are many strategies to measure how different climate changes affect soil erosion globally, how land use and conservation strategies may be able to lessen these effects, and how uncertain these effects are.

With a mean value of 61 tons/ha/year, the estimated potential soil loss in the study area ranged from 0 to 4615 tons/ha/year, as shown in Figure 15.

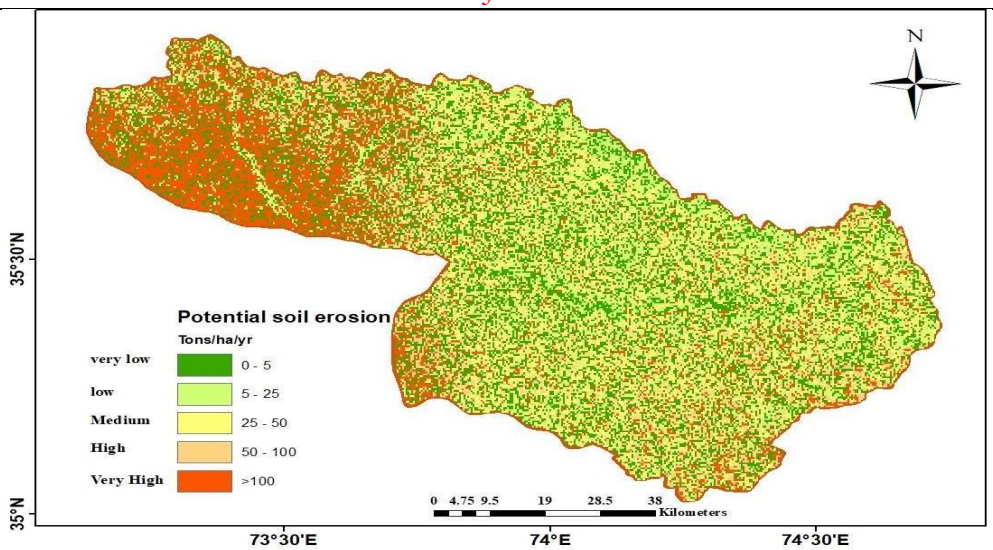

Figure 15. Potential soil loss

Actual Soil Erosion Using Landsat Image

The actual soil loss (Figure 16) was calculated using the RUSLE five factors, with a mean value of 27 tons/ha/year; the projected actual average yearly soil loss is 2279.3 tons/ha/year. The total area under the very low, low, moderate, high, and very high categories has changed by 32%, 36%, 17%, 10%, and 5%, respectively (Table 3). The spatial distribution of soil loss shown in Figure 17 is the graphical representation.

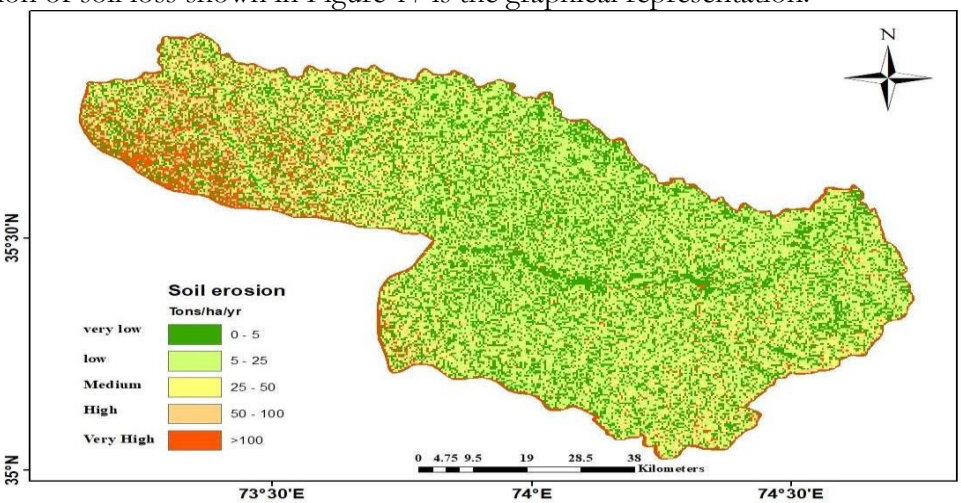

Figure 16. Actual soil loss

Table 3. Soil erosion area in percentage

Soil Erosion tons/ha/yr		Area in percentage
Very low	Less than 5	32%
Low	5-25	36%
Moderate	25-50	17%
High	50-100	10%
Very High	>100	5%

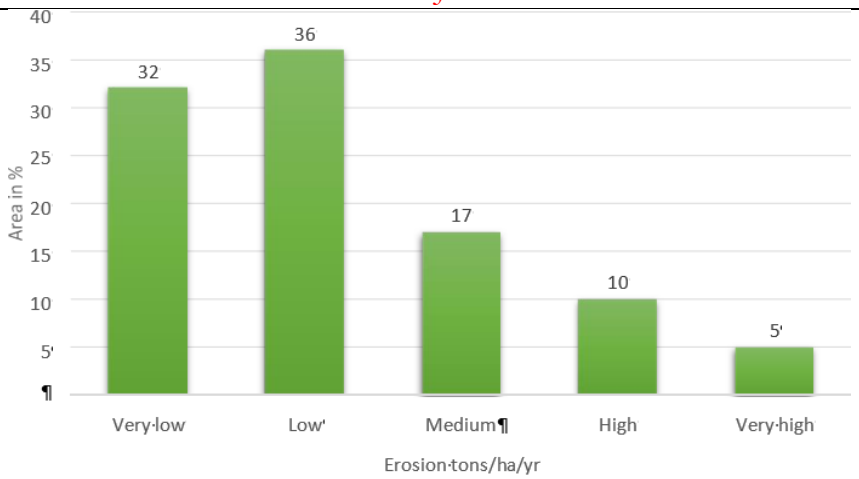

Figure 17. Percentage coverage of the erosion risk zone

Soil Erosion in Different Slope and Elevation Zones:

Soil erosion varies across different slopes and elevation zones. Figure 18 shows that in four slope classes ranging from <5, 5-10, 10-30, and greater than 30, the mean soil loss is 14.5, 18.7, 24.9, and 31.3 tons/ha/yr, respectively. The soil loss was recorded as low on a slope less than 5, and it is higher on a slope greater than 30. The area has a maximum slope of 67 degrees.

Soil erosion was also calculated for elevation zones (meters) from <2000, 2000-3000, 3000-4000, 4000-5000, 5000-6000, and >6000 (Figure 19). Soil erosion in six classes of elevation was 21.5, 24.4, 32.7, 25.9, 27.4, and 30.7 tons/ha/yr, respectively. Soil erosion was minimal in the <2000 zone and maximal in the 3000-4000 elevation zone..

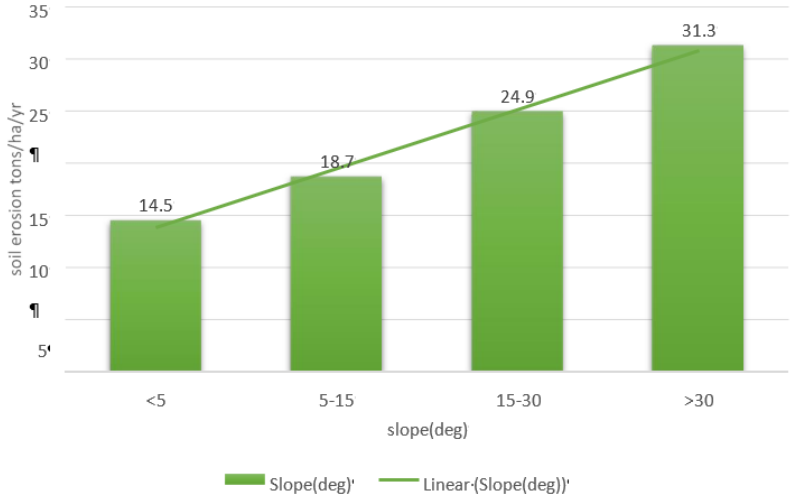

Figure 18. Average erosion rates on different slopes

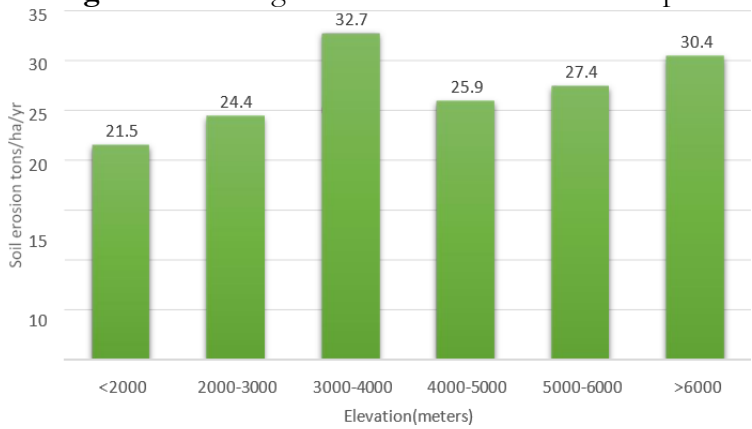

Figure 19. Soil erosion at different elevation zones

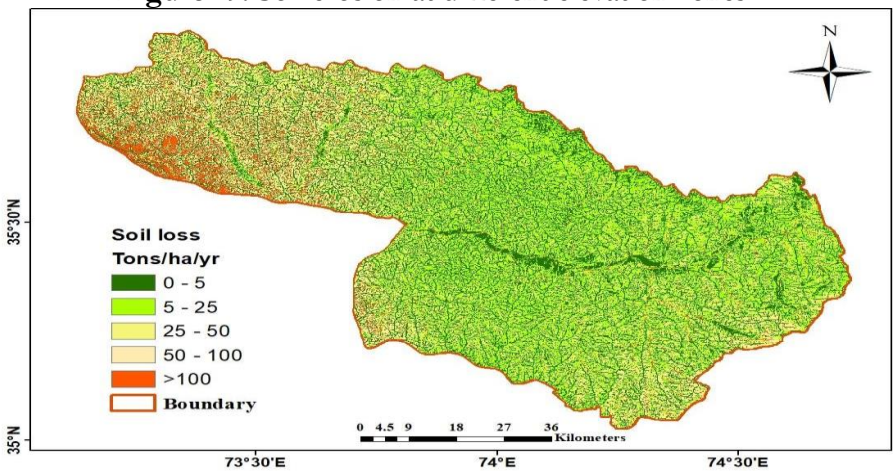

Figure 20. Soil erosion map using Sentinel-2

Actual Soil Erosion Using Sentinel-2 Images

The actual soil loss was also calculated using Sentinel-2 images, with a mean value of 26 tons/ha/year; the projected actual average yearly soil loss is 4636.7 tons/ha/year. The total area under the very low, low, moderate, high, and very high categories has changed by 32%, 36%, 17%, 10%, and 5%, respectively. The spatial distribution of soil loss is shown in Figure 20.

Discussion:

The findings of this study highlight the significant influence of rainfall erosivity (R), soil erodibility (K), slope length and steepness (LS), and cover management (C) on soil loss in the Diamer region. The R factor, which measures the erosive potential of rainfall, demonstrated a spatially variable pattern across the study area. Previous research has emphasized that rainfall intensity and volume are the dominant drivers of erosion [28][29]. In the current study, higher erosivity values were recorded in the western parts of the district, which correspond with regions experiencing greater rainfall intensity. These results confirm that intense precipitation events remain the primary determinants of soil detachment and transport, consistent with observations from other mountainous regions [29].

Soil erodibility (K), influenced by soil texture, structure, organic matter, and permeability, also played a critical role in erosion susceptibility. The calculated K values in this study ranged between 0.15- and 0.18-tons ha h ha^{-1} MJ^{-1} mm^{-1}, with an average of 0.159, suggesting moderate erodibility of the local soils. This aligns with findings by [30], who noted that soils with medium texture and low organic matter content are more prone to detachment. The distribution of soil mapping units further revealed that shallow and calcareous soils on mountain slopes were particularly vulnerable, reflecting the structural weaknesses of thin soil profiles in steep terrain.

Topographic influences, measured through the LS factor, showed a strong positive correlation with erosion rates. As expected, steeper slopes and longer slope lengths amplified runoff velocity and erosive power, leading to increased soil loss [31]. In Diamer, soil erosion rates were significantly higher on slopes exceeding 30°, where the mean erosion reached 31.3 tons/ha/yr, compared to only 14.5 tons/ha/yr on slopes below 5°. This relationship highlights the importance of slope stabilization measures in reducing erosion risks in mountainous areas.

The cover management factor (C) was also found to exert substantial control over soil erosion. Vegetation covers significantly reduced soil detachment, with lower C values (0.001–0.2) associated with croplands and forests, while higher C values (>0.5) corresponded to barren land and water bodies. The NDVI-derived C factor confirmed this relationship, indicating that vegetation cover remains the most effective natural barrier against erosion, a finding consistent

with [32]. Thus, areas with sparse vegetation or seasonal land use changes are more exposed to erosion hazards.

When the combined effect of R, K, LS, and C was considered through the RUSLE model, the mean actual soil erosion was estimated at 27 tons/ha/yr, placing the majority of the study area in the "moderate to high" erosion category [15]. This value is higher than those reported for the Sub-Himalayan region (8.4 tons/ha/yr; [27] and Azad Jammu Kashmir (22.25 tons/ha/yr; [33], but lower than estimates from the Hindu Kush (41.9 tons/ha/yr) and Himalaya (21.1 tons/ha/yr). Such variation reflects the combined effects of steep terrain, variable rainfall distribution, and heterogeneous land use in Diamer.

Correlation analysis further strengthened these findings. Pearson's correlation coefficients indicated a strong positive relationship between the C factor and soil erosion ($r = 0.94$) and between the LS factor and soil erosion ($r = 0.83$), while NDVI showed a strong negative correlation with erosion ($r = –0.77$). These results reinforce the critical role of vegetation cover and slope conditions in regulating soil loss processes, consistent with earlier studies [34][1].

Overall, the discussion confirms that Diamer's vulnerability to soil erosion is largely controlled by steep topography, high rainfall erosivity, and inadequate vegetation cover. Without targeted soil conservation strategies such as terracing, afforestation, and land-use regulation, soil degradation may intensify under projected climate change and land use dynamics.

Limitations and Strengths:

The RUSLE model is the most useful tool for estimating soil loss. This model is the best choice for developing countries with limited data since it can forecast soil loss with minimal information. Other models are complex and challenging to understand, and there is a high potential for errors, while RUSLE provides an easy and adaptable method for determining soil loss. However, it was developed using U.S. datasets; estimating soil erosion solely by multiplying different parameters would not provide an accurate result since aspects like routing and sediment deposition are not taken into account [35].

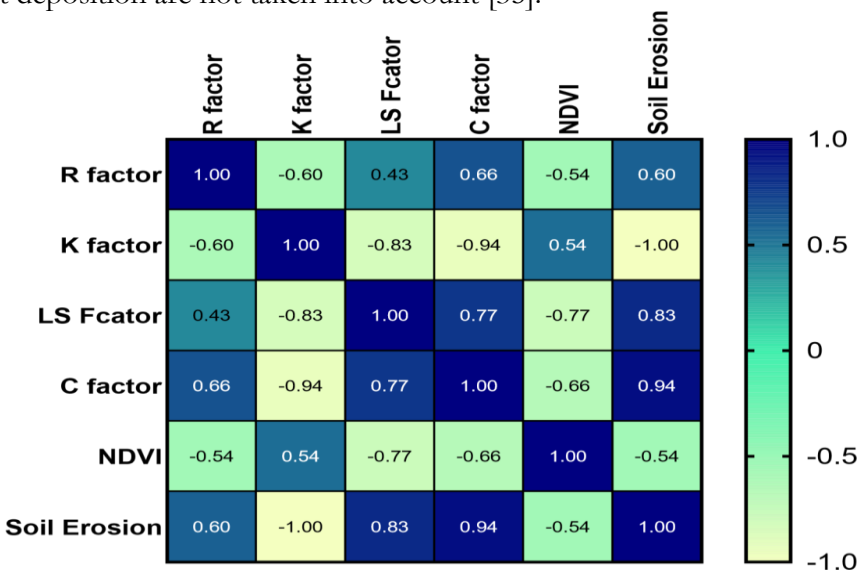

Figure 21. Pearson Correlation

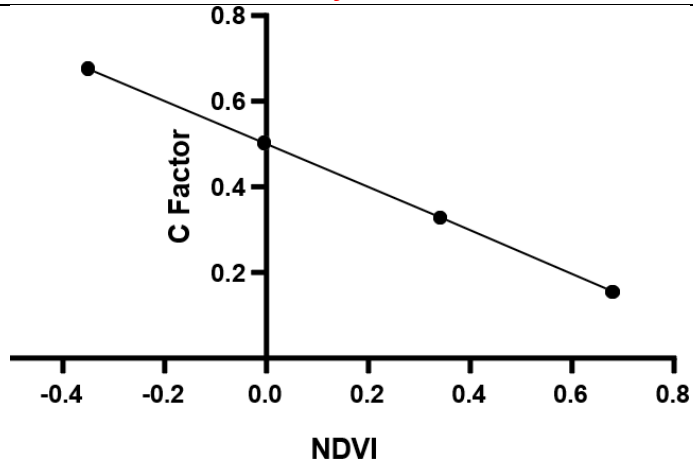

Figure 22. Correlation coefficient

The C factor and soil erosion show a highly significant correlation (0.94). Likewise, the LS factor and soil erosion show a highly significant correlation (0.83). The LS factor and NDVI have a strong negative correlation (-0.77) as shown in Figure 22.

Conclusion:

Using five factors, the long-term average annual mean of soil loss on slopes is estimated using the empirically based modeling approach known as RUSLE. It calculates soil loss based on comparable topography and climate conditions. The evaluation of soil erosion severity uses the RUSLE equation based on GIS that takes crop management, rainfall, soil, and DEM into account. Based on the degree of soil erosion, there are five categories for the rate. Five percent of the area is considered to be in severe danger, and 95% of the area is considered low-risk. Selected field surveys and ground truthing, covering large areas, are advantages of the NDVI-based C factor. However, there are some drawbacks, such as limited exposure to specific factors that determine the C factor, such as canopy structure and vegetation cover health. On the other hand, the C factor mapping method, which uses the NDVI, satisfies the need to reduce field survey costs quickly. NDVI and RUSLE values seem to have a negative correlation, which means that the higher the mean NDVI values, the lower the RUSLE values. This indicates that the higher the precipitation levels, the higher the expected erosion during that period. This result is consistent with previous research showing a negative relationship between vegetation and soil erosion. The amount of time needed to retrieve, download, and prepare images was greatly reduced by the GEE platform. The amount of time needed to retrieve, download, and prepare imagery was greatly reduced by using the GEE platform, as it provides data that is already calibrated and geometrically corrected. Uploading data to the cloud and integrating it with existing material can be a highly convenient and quick operation if data is unavailable in GEE's databases. Process automation is possible thanks to GEE's IDE, which enables users to create their programming scripts to reduce computational time and effort. Uploading data to the cloud and integrating it with existing data can be a highly convenient and quick operation if data is unavailable in GEE's databases. Process automation is possible thanks to GEE's IDE, which enables users to create their programming scripts to reduce computation time and effort. The evaluation of the erosion impact of different agricultural systems and conservation support practices is aided by the comparison of potential and actual soil loss. The study also demonstrates that areas with higher rainfall are more susceptible to soil loss since the degree of rainfall erosivity and the rate of soil loss are closely correlated. The methodology for mapping and estimating various RUSLE parameters could also be useful for other similar studies. Additionally, this study demonstrates how effectively GIS and RUSLE methodologies work to develop the spatial pattern of soil erosion. Decision-makers may find similar estimates of projected soil loss and their spatial distribution useful in larger-scale planning and developing

soil conservation strategies at the regional level.

References:

[1] K. H. Jodhani, D. Patel, N. Madhavan, and S. K. Singh, "Soil Erosion Assessment by RUSLE, Google Earth Engine, and Geospatial Techniques over Rel River Watershed, Gujarat, India," *Water Conserv. Sci. Eng.*, vol. 8, no. 1, pp. 1–17, Dec. 2023, doi: 10.1007/S41101-023-00223-X/METRICS.

[2] C. S. P. O. Shishant Gupta, "Pixel-Based Soil Loss Estimation and Prioritization of North-Western Himalayan Catchment Based on Revised Universal Soil Loss Equation (RUSLE)," *Sustainability*, vol. 15, no. 20, p. 15177, 2023, doi: https://doi.org/10.3390/su152015177.

[3] D. V. V. Narayana and R. Babu, "Estimation of Soil Erosion in India," *J. Irrig. Drain. Eng.*, vol. 109, no. 4, pp. 419–434, Dec. 1983, doi: 10.1061/(ASCE)0733-9437(1983)109:4(419).

[4] M. S. B. Alam, Shaista, Ambreen Fatima, "Sustainable development in Pakistan in the context of energy consumption demand and environmental degradation," *J. Asian Econ.*, vol. 18, no. 5, pp. 825–837, 2007, doi: https://doi.org/10.1016/j.asieco.2007.07.005.

[5] P. S. Sanjay K. Jain, "Assessment of sedimentation in Bhakra Reservoir in the western Himalayan region using remotely sensed data," *Hydrol. Sci. J.*, vol. 47, no. 2, pp. 203–212, 2002, doi: https://doi.org/10.1080/02626660209492924.

[6] W. Peng, Z. Zhang, and K. Zhang, "Hydrodynamic characteristics of rill flow on steep slopes," *Hydrol. Process.*, vol. 29, no. 17, pp. 3677–3686, Aug. 2015, doi: 10.1002/HYP.10461;JOURNAL:JOURNAL:10991085.

[7] H. Gilani, A. Ahmad, I. Younes, and S. Abbas, "Estimation of annual soil erosion dynamics (2005 - 2015) in Pakistan using Revised Universal Soil Loss Equation (RUSLE)," *Authorea Prepr.*, Jan. 2021, doi: 10.22541/AU.160946369.92099648/V1.

[8] I. Rahim, S. M. Ali, M. Aslam, I. Rahim, S. M. Ali, and M. Aslam, "GIS Based Landslide Susceptibility Mapping with Application of Analytical Hierarchy Process in District Ghizer, Gilgit Baltistan Pakistan," *J. Geosci. Environ. Prot.*, vol. 6, no. 2, pp. 34–49, Feb. 2018, doi: 10.4236/GEP.2018.62003.

[9] A. & F. Ahmad, D., Hafeez, F., Irshad, M., Mehmood, Q., Tahir, A. A., Iqbal, "Gilgit-Baltistan," *Arab. J. Geosci.*, vol. 13, p. 1286, 2020.

[10] Kenneth Hewitt, "Catastrophic landslides and their effects on the Upper Indus streams, Karakoram Himalaya, northern Pakistan," *Geomorphology*, vol. 26, no. 1–3, pp. 47–80, 1998, doi: https://doi.org/10.1016/S0169-555X(98)00051-8.

[11] C. Hawas Khan, Muhammad Shafique, Muhammad A. Khan, Mian A. Bacha, Safeer U. Shah, Calligaris, "Landslide susceptibility assessment using Frequency Ratio, a case study of northern Pakistan," *Egypt. J. Remote Sens. Sp. Sci.*, vol. 22, no. 1, pp. 11–24, 2019, doi: https://doi.org/10.1016/j.ejrs.2018.03.004.

[12] P. Thapa, "Spatial Estimation of Soil Erosion Using RUSLE Modeling: A case study of Dolakha District, Nepal," Jul. 2020, doi: 10.21203/RS.3.RS-25478/V4.

[13] A. A. Karim, F., Ashraf, M. I., Amin, M., Khan, M. R., & Khan, "Impact of climatic factors on land-use changes using geo-spatial techniques," *J. Appl. Agric. Biotechnol.*, vol. 1, no. 2, pp. 58–68, 2016, [Online]. Available: https://www.researchgate.net/publication/344538415_Impact_of_climatic_factors_on_land-use_changes_using_geo-spatial_techniques

[14] D. . Wischmeier, W.H. and Smith, "Predicting Rainfall Erosion Losses," *A Guid. to Conserv. Planning. USDA Agric. Handb.*, 1978, [Online]. Available: https://www.scirp.org/reference/referencespapers?referenceid=1687723

[15] A. Ashraf and I. Ahmad, "Evaluation of soil loss severity and ecological restoration approach for sustainable agriculture in the Hindu Kush, Karakoram and Himalaya

region," *J. Mt. Sci.*, vol. 21, no. 5, pp. 1509–1521, May 2024, doi: 10.1007/S11629-023-8385-Y/METRICS.

[16] S. Ghosh, "An Assessment of RUSLE Model and Erosion Vulnerability in the Slopes of Dwarka–Brahmani Lateritic Interfluve, Eastern India," *Clim. Environ. Disaster Dev. Ctries.* , pp. 475–506, 2022, doi: 10.1007/978-981-16-6966-8_26.

[17] D. K. McCool, L. C. Brown, G. R. Foster, C. K. Mutchler, and L. D. Meyer, "Revised Slope Steepness Factor for the Universal Soil Loss Equation," *Trans. ASAE*, vol. 30, no. 5, pp. 1387–1396, Sep. 1987, doi: 10.13031/2013.30576.

[18] B. LE Moore, I. D, Turner AK, Wilson JP, Jenson SK, "GIS and land-surface-subsurface process modeling," *Goodchild MF Environ. Model. with GISOxford Univ. Press. U.K*, 1993, [Online]. Available: https://www.researchgate.net/publication/246324435_GIS_and_land-surface-subsurface_process_modeling

[19] K. Ghosal and S. Das Bhattacharya, "A Review of RUSLE Model," *J. Indian Soc. Remote Sens.*, vol. 48, no. 4, pp. 689–707, Apr. 2020, doi: 10.1007/S12524-019-01097-0/METRICS.

[20] M. A. Rather, J. Satish Kumar, M. Farooq, and H. Rashid, "Assessing the influence of watershed characteristics on soil erosion susceptibility of Jhelum basin in Kashmir Himalayas," *Arab. J. Geosci.*, vol. 10, no. 3, pp. 1–25, Feb. 2017, doi: 10.1007/S12517-017-2847-X/METRICS.

[21] G. R. C. Nazir Ahmad, "Irrigated Agriculture of Pakistan," *Groundwater*, 1988, [Online]. Available: https://books.google.com.pk/books/about/Irrigated_Agriculture_of_Pakistan.html?id=Fn4_AAAAYAAJ&redir_esc=y

[22] J. A. Oliveira, J. M. L. Dominguez, M. A. Nearing, and P. T. S. Oliveira, "A GIS-Based procedure for automatically calculating soil loss from the universal soil loss Equation: GISus-M," *Appl. Eng. Agric.*, vol. 31, no. 6, pp. 907–917, 2015, doi: 10.13031/AEA.31.11093.

[23] V. L. D. Daniel Fonseca de Carvalho, "Predicting soil erosion using Rusle and NDVI time series from TM Landsat 5," *Pesqui. Agropecu. Bras.*, 2014, doi: 10.1590/S0100-204X2014000300008.

[24] I. Z. G. S. Papaiordanidis, "Soil erosion prediction using the Revised Universal Soil Loss Equation (RUSLE) in Google Earth Engine (GEE) cloud-based platform," *Bull. V.V. Dokuchaev Soil Inst.*, 2019, doi: https://doi.org/10.19047/0136-1694-2019-100-36-52.

[25] C. L. Arnold and C. J. Gibbons, "Impervious Surface Coverage: The Emergence of a Key Environmental Indicator," *J. Am. Plan. Assoc.*, vol. 62, no. 2, pp. 243–258, 1996, doi: 10.1080/01944369608975688.

[26] S. T. Pooja Koirala, "Estimation of Soil Erosion in Nepal Using a RUSLE Modeling and Geospatial Tool," *Geosciences*, vol. 9, no. 4, p. 147, 2019, doi: https://doi.org/10.3390/geosciences9040147.

[27] A. Ashraf, "Risk modeling of soil erosion under different land use and rainfall conditions in Soan river basin, sub-Himalayan region and mitigation options," *Model. Earth Syst. Environ.*, vol. 6, no. 1, pp. 417–428, Mar. 2020, doi: 10.1007/S40808-019-00689-6/METRICS.

[28] R. Lal, "Soil Erosion in the Tropics: Principles and Management," *McGraw Hill*, vol. 588, 1990, [Online]. Available: https://www.scirp.org/reference/referencespapers?referenceid=2193850

[29] A. Khan, A. U. Rahman, and S. Mahmood, "Spatial estimation of soil erosion risk using RUSLE model in District Swat, Eastern Hindu Kush, Pakistan," *J. Water Clim. Chang.*,

vol. 14, no. 6, pp. 1881–1899, Jun. 2023, doi: 10.2166/WCC.2023.495/1246359/JWC0141881.PDF.

[30] S. R. Kashiwar, M. C. Kundu, and U. R. Dongarwar, "Soil erosion estimation of Bhandara region of Maharashtra, India, by integrated use of RUSLE, remote sensing, and GIS," *Nat. Hazards*, vol. 110, no. 2, pp. 937–959, Jan. 2022, doi: 10.1007/S11069-021-04974-5/METRICS.

[31] B. J. B. and J. C. H. C.T. Haan, "Design Hydrology and Sedimentology for Small Catchments," *Elsevier*, 1994, [Online]. Available: https://www.sciencedirect.com/book/9780123123404/design-hydrology-and-sedimentology-for-small-catchments

[32] V. Prasannakumar, R. Shiny, N. Geetha, and H. Vijith, "Spatial prediction of soil erosion risk by remote sensing, GIS and RUSLE approach: A case study of Siruvani river watershed in Attapady valley, Kerala, India," *Environ. Earth Sci.*, vol. 64, no. 4, pp. 965–972, Oct. 2011, doi: 10.1007/S12665-011-0913-3/METRICS.

[33] H. Gilani, A. Ahmad, I. Younes, and S. Abbas, "Impact assessment of land cover and land use changes on soil erosion changes (2005–2015) in Pakistan," *L. Degrad. Dev.*, vol. 33, no. 1, pp. 204–217, Jan. 2022, doi: 10.1002/LDR.4138.

[34] C.-U. Hwang, Chang-Su ; Kim, Kyung-Tag, Oh, Che-Young ; Jin, Cheong-Gil, Choi, "A Study on Correlation between RUSLE and Estuary in Nakdong River Watershed," *J. Korean Soc. Geospatial Inf. Sci.*, vol. 18, no. 3, pp. 3–10, 2010, [Online]. Available: https://koreascience.kr/article/JAKO201019547057082.pub?&lang=en

[35] M. K. L. Muhammad Waseem, Fahad Iqbal, Muhammad Humayun, Muhammad Umais Latif, Tayyaba Javed, "Spatial Assessment of Soil Erosion Risk Using RUSLE Embedded in GIS Environment: A Case Study of Jhelum River Watershed," *Appl. Sci.*, vol. 13, no. 6, p. 3775, 2023, doi: https://doi.org/10.3390/app13063775.